Protein Phosphatase 2A and Rapamycin Regulate the Nuclear Localization and Activity of the Transcription Factor GLI3

Sybille Krauß,[1,2] John Foerster,[4] Rainer Schneider,[2,3] and Susann Schweiger[2,4]

[1]Charité University Hospital, Department of Dermatology and [2]Max-Planck Institute for Molecular Genetics, Berlin, Germany; [3]Institute of Biochemistry and Center for Molecular Biosciences Innsbruck, Innsbruck, Austria; and [4]Ninewells Hospital, Department of Neuroscience and Pathology, Scotland, United Kingdom

Abstract

Gain-of-function alterations to the sonic hedgehog (SHH) signaling cascade have been found in a wide range of tumors. Three SHH effectors, GLI1, GLI2, and GLI3, regulate transcription of diverse genes involved in cell growth and cell proliferation. Here, we show that protein phosphatase 2A (PP2A), its regulatory subunit, α4, and rapamycin, an inhibitor of the mammalian target of rapamycin kinase complex 1 (mTORC1), regulate the nuclear localization and transcriptional activity of GLI3. An increase in PP2A activity or treatment with rapamycin leads to cytosolic retention of GLI3 and, consequently, reduced transcription of the GLI3 target gene and cell cycle regulator, *cyclin D1*. Conversely, inhibition of PP2A results in increased expression of *cyclin D1*. In summary, our findings reveal the existence of a hitherto unrecognized molecular cross-talk between the oncogenic SHH pathway and the tumor suppressor PP2A and suggest a novel mechanism underlying the anticancerogenic effects of rapamycin. [Cancer Res 2008;68(12):4658–65]

Introduction

Gain-of-function alterations to sonic hedgehog (SHH) signaling are associated with tumor formation. For example, mutations in the SHH receptor Patched1 (PTC1), the transmembrane protein Smoothened, and the transcription factor GLI1 are found in basal cell carcinoma, glioblastoma, osteosarcoma, or bladder carcinoma (reviewed in ref. 1). In addition, autonomous activation of the SHH pathway has been shown in tumors of the digestive tract (2), small cell lung cancer (3), pancreatic carcinomas (4), and prostate cancer (5).

The SHH signal response is mediated by the transcriptional effectors GLI1, GLI2, and GLI3, which are orthologues of the *Drosophila* transcription factor Cubitus interruptus (Ci). In *Drosophila*, Ci is part of a large, microtubule-associated protein complex containing the serine/threonine kinase Fused, the kinesin-related protein Costal2, and Suppressor of Fused. In the absence of Hh signaling, Ci becomes phosphorylated and is then proteolytically cleaved into two fragments; the NH_2 terminal peptide translocates into the nucleus, serving as a transcriptional repressor of Hh target genes. In the presence of Hh signaling, Ci processing is prevented, the protein complex dissociates from microtubules, and full-length Ci translocates into the nucleus, where it functions as a transcriptional activator of Hh target genes (reviewed in ref. 6). Like Ci, GLI3 undergoes phosphorylation-dependent cleavage and acts as either a transcriptional repressor or activator, depending on the SHH activation status of vertebrate cells (reviewed in ref. 7). GLI3 either regulates SHH target genes directly or activates the transcription of GLI1, which acts as a pure transcriptional activator, inducing its target genes (8). The outcome of SHH signaling depends critically on the regulation of GLI3 cleavage and the nuclear entry of noncleaved GLI3. However, the factors regulating these events remain incompletely understood.

Protein phosphatase 2a (PP2A) has been implicated as a negative regulator of tumor growth due to its interaction with oncoproteins and its regulatory involvement in cell migration. Moreover, the PP2A inhibitor okadaic acid is a potent tumor promoter (reviewed in ref. 9). The mechanisms underlying this function have not been uncovered. PP2A acts in opposition to the kinase mammalian target of rapamycin complex 1 (mTORC1). Both enzymes control the phosphorylation status and, thereby, the activity of the ribosomal S6 kinase (S6K) and initiation factor 4E binding protein (4E-BP), two key proteins of mammalian translation (reviewed in ref. 10). mTOR exists in mammalian cells either in the rapamycin-sensitive mTORC1 together with the proteins Raptor and mLST8 or in the rapamycin-insensitive mTORC2 with Rictor, Sin1, and mLST8 (reviewed in ref. 11).

The activity of PP2A itself is tightly regulated. In yeast, TOR kinase directly phosphorylates the Tap42 protein, which then forms a complex with the C subunit of PP2A, thus displacing it from the A and B subunits and thereby inhibiting PP2A activity (reviewed in ref. 12). In mammals, the catalytic PP2A subunit, PP2Ac, is targeted for ubiquitin-mediated proteolytic degradation by the ubiquitin ligase MID1, which contacts PP2A through the mammalian Tap42 orthologue α4 (13).

The drug rapamycin has been shown to act as an antineoplastic in addition to having an immunosuppressive function. Several lines of evidence suggest that this antineoplastic effect may be linked to its interference with mTORC1 activation. First, rapamycin inhibits the kinase activity of mTORC1 by direct binding (reviewed in ref. 14). Second, rapamycin causes dissociation of the catalytic subunit (PP2Ac) from the regulatory subunit α4 (15–18), allowing PP2Ac to act on the mTORC1 targets S6K and 4E-BP. Third, rapamycin inhibits mTORC1 signaling by activating PP2A activity (15, 19).

Here, we show that PP2A and the mTORC1 inhibitor rapamycin regulate the nuclear localization of noncleaved, transcriptionally active GLI3 in cancer cell lines. Both inhibition of mTORC1 by rapamycin and activation of PP2A through inhibition of its MID1/α4-mediated degradation caused cytosolic retention of the SHH effector GLI3 and reduction of its transcriptional activation function toward *cyclin D1*. These data provide evidence for a shared molecular network comprising SHH and mTORC1/PP2A

Note: Supplementary data for this article are available at Cancer Research Online (http://cancerres.aacrjournals.org/).

Requests for reprints: Rainer Schneider, Institute of Biochemistry and Center for Molecular Biosciences Innsbruck, Peter-Mayr-Strasse 1a, 6020 Innsbruck, Austria. Phone: 0043-512-507-5273; Fax: 0043-512-507-96956; E-mail: rainer.schneider@uibk.ac.at.

doi:10.1158/0008-5472.CAN-07-6174

signaling and suggest a novel mechanism underlying the anti-cancerogenic effects of rapamycin.

Materials and Methods

Constructs. Constructs containing GLI3-cDNA coding for amino acids 1-1522 cloned into pEGFP-N1-vector (Clontech) and for amino acids 18-1549 cloned into pEGFP-C1-vector (Clontech) were kindly provided by Prof. K-H. Grzeschik. GLI3 cDNA coding for amino acids 18-1596 was cut out of the pBS vector containing full-length GLI3 cDNA, which was kindly provided by Prof. A. Vortkamp, using EcoRI (Fermentas), and ligated into the multiple cloning site of the vectors pCMV-Tag2A and pCMV-Tag3A (Stratagene). The complete coding sequence of α4 was PCR-amplified and cloned into the $P_{EF\text{-}1a}$ promoter multiple cloning site of the pBudCE4 vector (Invitrogen) and into the multiple cloning site of the pCMVTag3A vector (Stratagene) using suitable restriction enzymes (see product information). The sequence corresponding to B-Box1 of the MID1 protein was PCR-amplified and ligated into the multiple cloning site of the vectors pCMVTag3A and pCMVTag2A (Stratagene). Complete GLI1 and mGLI2 coding sequences were PCR-amplified and cloned into the pCMVTag3A vector (Stratagene) using suitable restriction enzymes (see product information).

Cell fractionation. HeLa cells (8×10^5) were seeded and grown for 24 h. Transfections with the respective plasmids were performed using Polyfect transfection reagent (Qiagen) according to the manufacturer's instructions. Twenty-four hours after transfection, cells were resuspended in fractionation buffer [40 μg/mL digitonin, 50 mmol/L Tris-HCl (pH 7.5), 100 mmol/L NaCl, 2.5 mmol/L $MgCl_2$] and incubated for 10 min at room temperature. Nuclear and cytosolic fractions were separated by centrifugation (1,000 × *g*, 10 min, 4°C).

Immunofluorescence. For immunofluorescence experiments, HeLa cells were plated on coverslips at a density of 1×10^5 cells 1 d before transfection. Cells were transfected with the respective plasmids using Polyfect transfection reagent (Qiagen) according to the manufacturer's instructions. Twenty-four hours after transfection, cells were fixed with 3.7% paraformaldehyde in 1.2× PEM buffer [10× PEM contains 1 mol/L Pipes, 0.05 mol/L EGTA, 0.02 mol/L $MgCl_2$ (pH 7.0)]. Afterwards, cells were permeabilized with 0.2% Triton X-100 and blocked with 1% bovine serum albumin. Antibody incubations were carried out following the manufacturer's instructions. For PP2A and mTORC1 inhibition, cells were incubated with the respective substances as follows: rapamycin (Sigma) at final concentration from 0.5 pmol/L to 1 μmol/L for 1 h at 37°C, wortmannin at a final concentration of 0.1 μmol/L for 1 h at 37°C, fostriecin (Sigma) at a final concentration of 500 nmol/L for 1 h at 37°C, and okadaic acid at a final concentration of 100 nmol/L for 4 h. Cells were randomly chosen and counted independently by three individuals.

Antibodies. Anti-GFP was purchased from Roche, monoclonal anti–c-myc from Clontech, anti-FLAG from Stratagene, horseradish peroxidase (HRP) anti-rabbit from Amersham, HRP anti-mouse, Cy3 anti-mouse, Cy3 anti-rabbit, FITC anti-mouse, and FITC anti-rabbit from Dianova. Anti-Lamin A/C was purchased from Santa Cruz.

RNA interference. Twenty-four hours before transfection, HeLa cells were seeded into six-well plates at a density of 1×10^5. Cells were transfected with 1.3 μg of synthetic small interfering RNA (siRNA) per well using Oligofectamine (Invitrogen) according to the manufacturer's instructions. Transfection efficiencies were monitored with fluorescein-labeled control siRNA (Qiagen). Approximately, 95% of the cells showed siRNA uptake. The sequences of siRNAs are listed (Supplementary Table S3).

Real-time PCR. Twenty-four hours before treatment, HeLa cells were seeded at a density of 1×10^5 cells per well of a six-well plate. Cells were either treated with okadaic acid (final concentration in the culture medium, 100 nmol/L), fostriecin (500 nmol/L), or rapamycin (25 nmol/L) and incubated for 4 h or transfected with siRNA and incubated for 24 or 48 h. Total RNA was

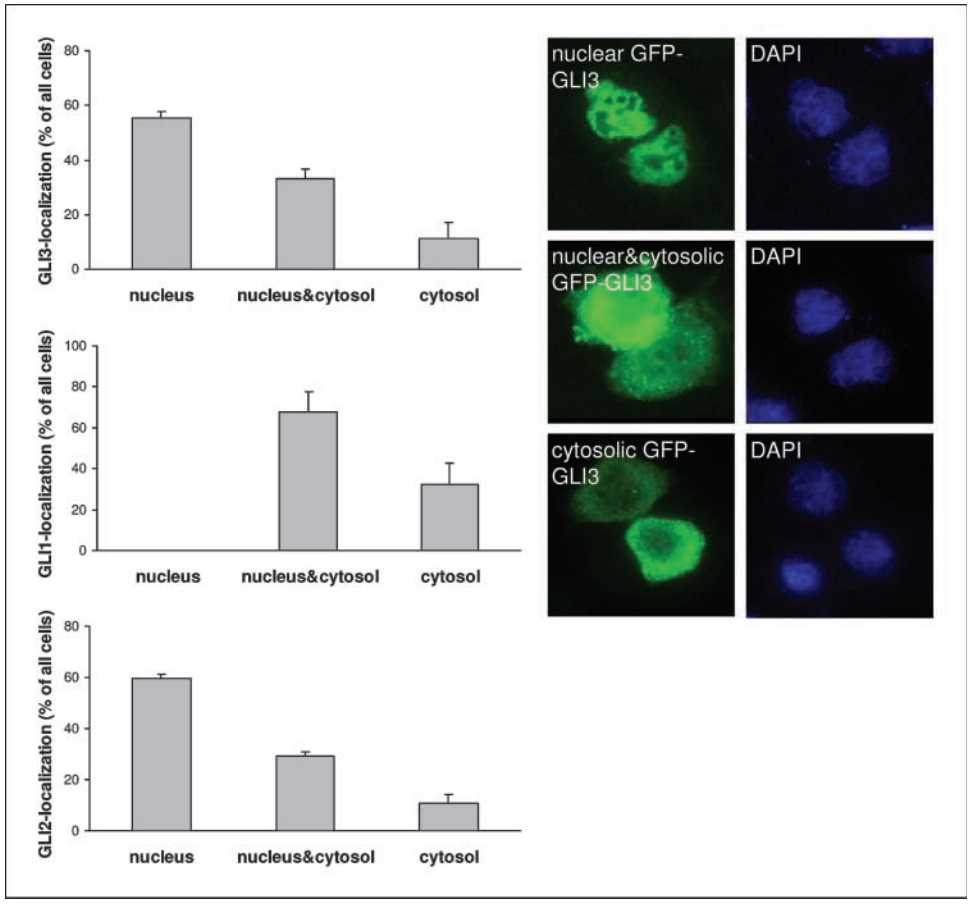

Figure 1. Subcellular localization of GLI proteins. Subcellular distribution of GFP-GLI3, myc-mGLI2, and myc-GLI1 in HeLa cells. *Right,* GFP-GLI3 signal distribution in individual cells occurred in three patterns: exclusively nuclear fluorescence (*top*), even staining throughout the cytosol and nucleus (*middle*), or predominantly cytosolic fluorescence (*bottom*). *Left,* transfected cells were randomly chosen and counted and classified in one of the three groups. The subcellular distribution of GFP-GLI3 (*top*), myc-mGLI2 (*middle*), and myc-GLI1 (*bottom*). *Columns,* mean scored per group from three independent experiments of 100 cells each; *bars,* SD.

isolated using an RNeasy Mini kit (Qiagen) following the manufacturer's instructions. cDNA was synthesized using the TaqMan reverse transcription reagents kit (Applied Biosystems), and real-time PCR was carried out using the SYBRGreen PCR master mix (Applied Biosystems) according to the manufacturer's instructions with an ABI 7900HT cycler under the following conditions: 50°C for 2 min; 95°C for 10 min; 95°C for 15 s, 60°C for 1 min for 40 cycles; and 95°C for 15 min, 60°C for 15 min, 95°C for 15 min for the dissociation stage. Primers used are listed (Supplementary Table S4).

Semiquantitative reverse transcription–PCR. Total RNA from different tumor cell lines was isolated using an RNeasy Mini kit (Qiagen) following the manufacturer's instructions. cDNA was synthesized using Superscript III reverse transcriptase (Invitrogen), and PCR was carried out using the Advantage 2 PCR enzyme system (BD Bioscience) according to the manufacturer's instructions. To amplify 18S RNA as an internal standard for quantification, we used QuantumRNA 18S Internal Standards (Ambion) following the manufacturer's protocol. Gene-specific primers used for amplification of *CCND1, GLI3*, and *PTC1* are listed (Supplementary Table S5).

Results

Autonomous expression of components of the SHH pathway in human tumor cell lines. Directed by the observation that gain-of-function alteration of SHH signaling, mTORC1 activation, and reduced PP2A activity contribute to tumorigenesis, we hypothesized that PP2A activity may interfere with activation of the SHH transcriptional effectors GLI1, GLI2, and GLI3 in tumor cell lines. To test this hypothesis, we first screened a range of tumor cell lines for expression of GLI3, the SHH receptor PTC1, and the SHH target *cyclin D1* (*CCND1*; refs. 20–23) to obtain a suitable model cell line with autonomously activated SHH-GLI signaling. Two melanoma cell lines (MeWo and SKMel29), three basal cell carcinoma cell lines (BCC-1, BCC-3, and BCC-5), a glioblastoma-astrocytoma cell line (U373MG), and cervix carcinoma cells (HeLa) all expressed the respective genes, suggesting there is constitutively active SHH signaling in these tumor-derived cells (Supplementary Fig. S1). To test whether this activation of the SHH pathway is indeed constitutive and independent of exogenous SHH ligand, we treated HeLa cells with SHH peptide or the SHH inhibitor cyclopamine. No differences in the expression of the three genes were seen in HeLa cells with and without SHH stimulation, suggesting SHH-independent expression of SHH pathway components in these cells.

GLI3, but not GLI1 or GLI2, subcellular localization depends on the PP2Ac-α4 protein complex. Because of their better transfection efficiencies, we chose HeLa and U373MG cells for subsequent experiments and confirmed the central findings in MeWo and SKMel29. Unfortunately, we were unable to transfect BCC cell lines with either plasmids or siRNA oligonucleotides with any of the protocols used. In the first set of experiments we tested whether the regulatory PP2A subunit α4 and/or rapamycin affect the subcellular localization of the GLI proteins. Overexpression of the α4 protein stabilizes the PP2Ac/α4/MID1 complex and increases PP2Ac degradation, whereas rapamycin induces PP2A activity. As shown for GFP-tagged GLI3 in Fig. 1, three different localization patterns of overexpressed GLI proteins were observed: predominantly nuclear, equally distributed in the nucleus and cytosol, or predominantly cytosolic. Overexpressed GFP-tagged GLI3 and myc-tagged mGLI2 (mouse GLI2) localized predominantly to the nucleus in the majority of transfected cells (55% and 60% of the cells, respectively). Myc-tagged GLI1, however, was found both in the nucleus and cytosol of most transfected cells (Fig. 1). Stabilization of the PP2A/α4/MID1 complex by overexpression of the α4 protein caused a significant shift of GLI3 to the nucleus but did not interfere with either mGLI2 or GLI1 subcellular localization (Fig. 2*A*). Similarly, treatment of GFP-GLI3 expressing cells with rapamycin markedly reduced the proportion of cells with predominantly nuclear GFP-GLI3 localization, whereas myc-GLI1 and

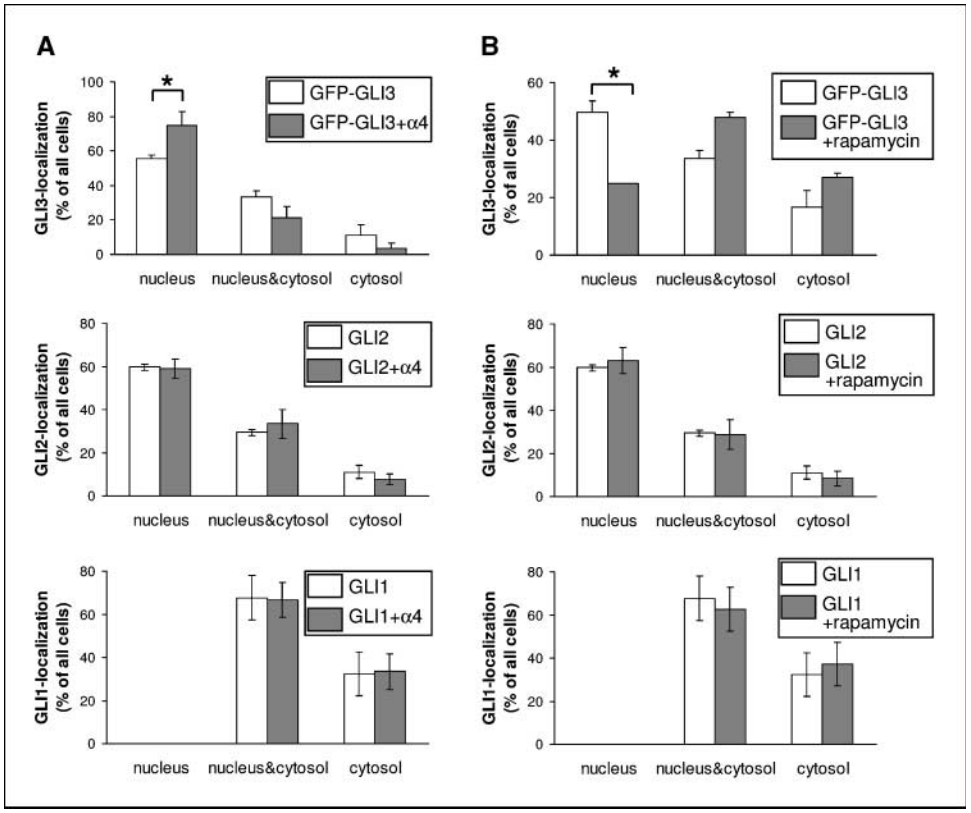

Figure 2. Subcellular localization of GLI proteins after manipulation of the MID1/PP2A complex and rapamycin treatment. *A,* subcellular localization of GFP-GLI3 (*top*), myc-mGLI2 (*middle*), and myc-GLI1 (*bottom*) in HeLa cells without further treatment (*white columns*) and after coexpression with α4-V5 (*gray columns*). Visualization and scoring were performed as described in the legend to Fig. 1. *t* test (two-tailed, homoscedastic): *, $P = 0.0146$. *B,* subcellular localization of GFP-GLI3 (*top*), myc-mGLI2 (*middle*), and myc-GLI1 (*bottom*) in HeLa cells without (*white columns*) or with treatment with 75 nmol/L rapamycin (*gray columns*) as determined by fluorescence microscopy. *t* test (two-tailed, homoscedastic): *, $P = 0.0109$.

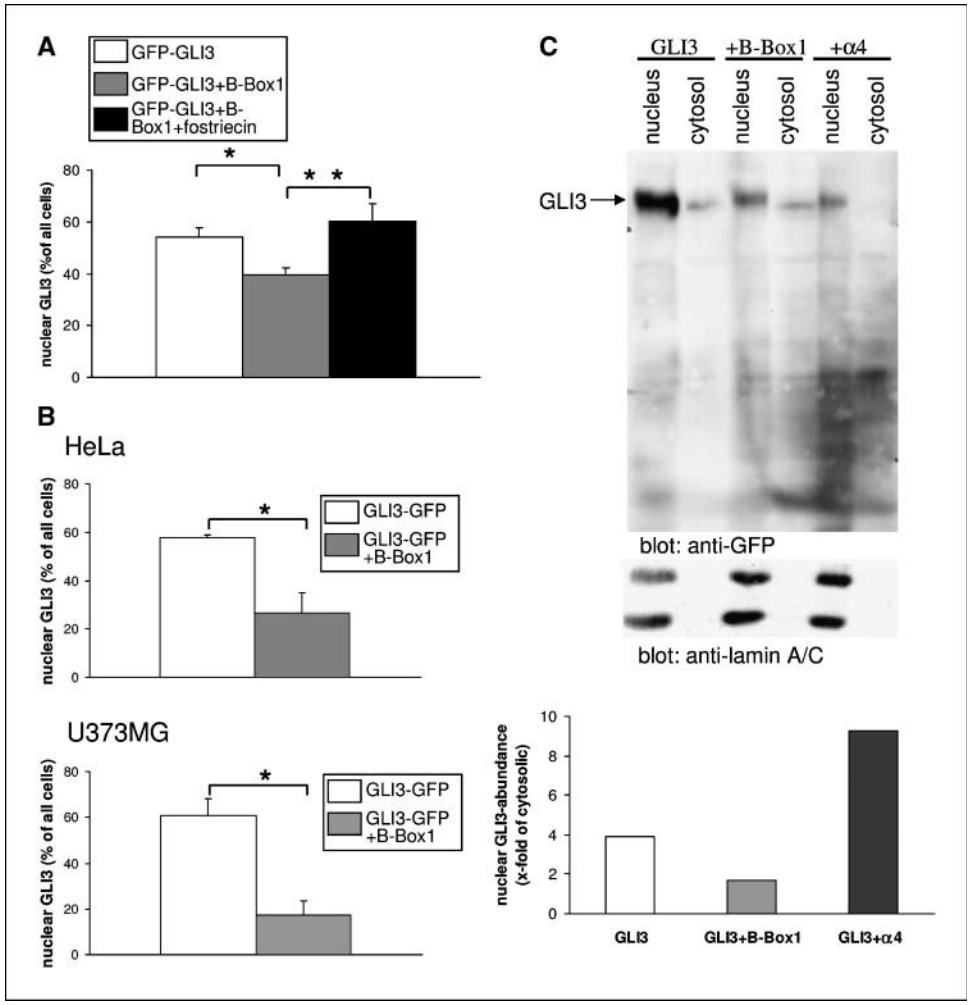

Figure 3. Subcellular localization of GLI3 after manipulation of the MID1/PP2A complex and rapamycin treatment. *A,* nuclear localization of GFP-GLI3 in HeLa cells expressing myc-B-Box1 in the absence (*gray column*) or presence (*black column*) of fostriecin. Visualization and scoring were performed as described in the legend to Fig. 1. *t* tests (two-tailed, homoscedastic): *, $P = 0.005$; **, $P = 0.008$. *B,* nuclear localization of GLI3-GFP in HeLa cells (*top*) and U373MG cells (*bottom*) without further treatment (*white columns*) and after coexpression with B-Box1 (*gray columns*). *t* test (two-tailed, homoscedastic): HeLa *, $P = 0.0029$, U373MG *, $P = 0.0015$. *C, top,* Western blot analysis of nuclear (*lanes 1, 3,* and *5*) and cytosolic (*lanes 2, 4,* and *6*) fractions from HeLa cells overexpressing GFP-GLI3 alone (*lanes 1* and *2*), GFP-GLI3 and myc-B-Box1 (*lanes 3* and *4*) or GFP-GLI3 and myc-α4 (*lanes 5* and *6*). Extracts were separated and analyzed with anti-GFP antibody (*top*). A specific signal was detected at the expected size of GFP-GLI3 (~220 kDa). Efficiency of cell fractionation was shown using an anti-lamin A/C antibody (*bottom*). The bands revealed by anti-GFP staining were quantified using the ImageQuant 5.2 software. *Bottom,* data represent relative abundance of nuclear GLI3 versus cytosolic GLI3 after the respective treatment. *White column,* GFP-GLI3 expression; *gray column,* coexpression with B-Box1; *black column,* coexpression with α4.

myc-mGLI2-expressing cells did not show any response to the treatment (Fig. 2*B*). Comparable results were obtained with COOH terminally GFP-tagged and NH_2 terminally FLAG-tagged or MYC-tagged GLI3 constructs, indicating that the observed effects were independent of protein cleavage and the specific nature of the overexpressed GLI3 fusion proteins (Supplementary Table S1*A*).

Overexpression of the MID1 B-Box1 domain disrupts the PP2Ac/α4/MID1 complex by competitive inhibition, leading to stabilization and activation of microtubule-associated PP2Ac (13).[5] Like rapamycin treatment, coexpression of GFP-GLI3 with B-Box1 caused a marked reduction of nuclear GLI3 accumulation (Fig. 3*A* and *B, gray columns*) in HeLa cells. Preincubation with fostriecin, a specific inhibitor of PP2A activity (24), fully abrogated the effect of B-Box1 on GFP-GLI3 localization (Fig. 3*A, black column*), confirming that the observed effect was indeed mediated via increased PP2A activity. A comparable effect of B-Box1 was seen in U373MG cells (Supplementary Table S1*A*) and with a COOH terminally tagged GLI3-GFP construct in both, HeLa and U373MG cells (Fig. 3*B*).

Western blot analysis of nuclear and cytosolic fractions of HeLa cells coexpressing GFP-GLI3 and myc-B-Box1, GFP-GLI3 and α4-V5, or GFP-GLI3 alone was performed to further corroborate the fluorescence microscopy data. As shown in Fig. 3*C*, the relative amount of GLI3 protein in nuclear versus cytosolic fractions was significantly increased upon coexpression of α4, whereas it decreased upon coexpression of B-Box1. No cleavage products were seen either in any of the cell fractions.

PP2A activity and rapamycin regulate GLI3 intracellular localization. The results presented thus far pointed at an important influence of PP2A activity on the subcellular localization of the SHH regulator GLI3. To verify this, we treated cells expressing GFP-GLI3 with the PP2A inhibitor okadaic acid. As expected, a significant increase of nuclear GFP-GLI3 was observed after okadaic acid treatment of HeLa cells (Fig. 4*A*). Analogous results were obtained in U373MG, MeWo, and SKMel29 cells (Supplementary Table S1B), thus demonstrating that the observed effect is operative in a variety of cancer cell lines.

We next determined whether the reduction of GLI3 nuclear localization observed in HeLa cells in response to rapamycin treatment (see above) is characteristic of tumor cells in general. To this end, we repeated the experiment in U373MG, MeWo, and SKMel29 cells. Cells overexpressing GFP-GLI3 were treated with rapamycin and subsequently analyzed for GFP-GLI3 localization by immunofluorescence. Indeed, a reduction in the number of cells with exclusively nuclear GLI3 localization was observed in all cell lines (Supplementary Table S1B). Rapamycin activates PP2A presumably by mTORC1-mediated displacement of α4 from the catalytic subunit of PP2A (16, 18, 25). In confirmation of an

[5] Unpublished data.

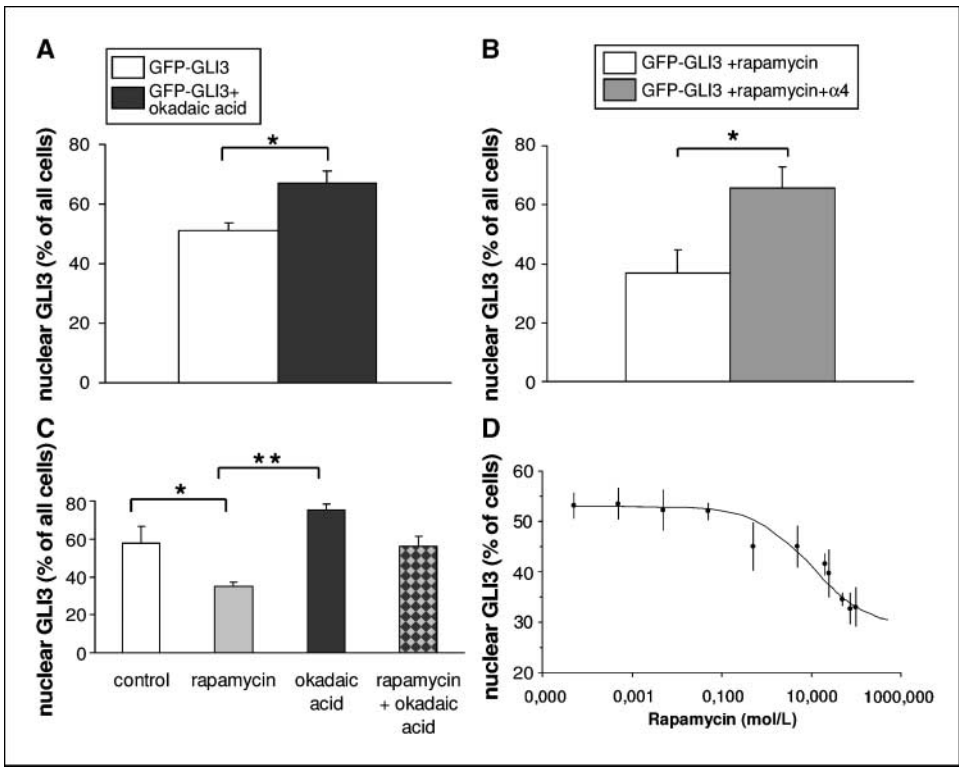

Figure 4. Subcellular localization of GLI3 and its dependency on PP2A activity. *A,* nuclear localization of overexpressed GFP-GLI3 in HeLa cells without (*white column*) or with treatment with 100 nmol/L okadaic acid (*black column*) as determined by fluorescence microscopy. Visualization and scoring were performed as described in the legend to Fig. 1. *t* test (two-tailed, homoscedastic): *, $P = 0.0044$. *B,* nuclear localization of overexpressed GFP-GLI3 in rapamycin-treated HeLa cells without (*white column*) or with coexpression of α4 (*gray column*). *t* test (two-tailed, homoscedastic): *, $P = 0.0097$. *C,* nuclear localization of overexpressed GFP-GLI3 in HeLa cells without (*white column*) or with rapamycin treatment (*gray column*), okadaic acid treatment (*black column*), or with combined treatment with rapamycin and okadaic acid (*patterned column*). *t* test (two-tailed, homoscedastic): *, $P = 0.0173$; **, $P = 0.0419$. *D,* nuclear localization of overexpressed GFP-GLI3 in HeLa cells after treatment with different amounts of rapamycin as determined by fluorescence microscopy. Data represent the relative percentage of cells with nuclear GLI3-signal. Visualization and scoring were performed as described in the legend to Fig. 1.

α4-dependent mode of action of rapamycin, the effect of rapamycin treatment on GLI3 localization could be rescued by overexpression of α4 (Fig. 4*B*). That rapamycin reduces GFP-GLI3 nuclear accumulation through activation of PP2A could further be shown by simultaneous treatment of cells with rapamycin and okadaic acid. As shown in Fig. 4*C*, inhibition of PP2A by okadaic acid caused a reversal of the rapamycin-induced cytosolic retention of GFP-GLI3 localization in the double-treated cells. By contrast, low-dose treatment with wortmannin, at concentrations that potently inhibit Akt and mTORC2-mediated signaling but have minimal effects on mTORC1 (26), had no detectable influence on the subcellular localization of GLI3 (Supplementary Fig. S2), suggesting an Akt and, hence, an mTORC2-independent mechanism.

We next analyzed the influence of rapamycin on the subcellular localization of GFP-GLI3 in a dose-response experiment. After stimulating GFP-GLI3 overexpressing cells with increasing concentrations of rapamycin, the subcellular localization of GFP-GLI3 was analyzed by immunofluorescence, and the IC_{50} value was determined (Fig. 4*D*). Intriguingly, the observed IC_{50} of 10 nmol/L is at the lower end of rapamycin serum concentration achieved clinically (27), suggesting that modulation of GLI3 transcriptional activity may also occur in patients being treated with rapamycin.

***Cyclin D1* expression depends on PP2A and mTORC1 activity.** To analyze the extent to which the expression of SHH target genes depends on active, nuclear GLI3, we knocked down GLI3 in HeLa cells using RNA interference (RNAi) and analyzed expression of a set of known tumor-related SHH target genes by real-time PCR. Similar results were obtained with two different RNAi oligonucleotides matching independent sequences of GLI3 (Supplementary Fig. S3 and data not shown). Whereas several of these target genes turned out not to be detectable in HeLa cells at the conditions used (Supplementary Table S2), others that were expressed did not respond to GLI3 knockdown, suggesting that GLI3 has no direct transcriptional effect on those genes in HeLa cells (Supplementary Fig. S3). In contrast, a surprisingly clear down-regulation of the cell cycle regulator *cyclin D1* was detected upon GLI3 knockdown, confirming that expression of *cyclin D1* is dependent on active GLI3 in our model system (Supplementary Fig. S3). Similar effects on the *cyclin D1* expression were also seen after GLI3 knockdown in U373MG, MeWo, and SKMel29 cells, suggesting a general dependence of *cyclin D1* transcription on a GLI3-mediated activation in tumor cells (Fig. 5). Again, experiments were performed with two different RNAi oligonucleotides matching independent sequences of GLI3.

Finally, because the subcellular localization of full-length GLI3 protein is regulated by PP2A activity and rapamycin, we asked whether the regulation of GLI3 localization by PP2A and rapamycin affects the transcriptional activity of GLI3. To this end, we analyzed the expression of the target gene *cyclin D1* either upon PP2A activation/mTORC1 inactivation (mediated by rapamycin) or upon inhibition of PP2A by its inhibitors okadaic acid and fostriecin using real-time PCR. As shown in Fig. 6*A*, PP2A activation/mTORC1 inhibition by rapamycin caused a large decrease in *cyclin D1* expression. Likewise, inhibition of PP2A activity by okadaic acid and fostriecin led to a clear up-regulation of *cyclin D1* expression. Thus, nuclear depletion of GLI3 by rapamycin correlates with a reduction in transcriptional activity of GLI3. PP2A dependence of the rapamycin effect on the *cyclin D1* expression could be shown by simultaneous treatment of cells with rapamycin and okadaic acid. According to the rescue effect seen in the localization experiment (Fig. 4*C*), *cyclin D1* expression in the double-treated cells resembled that in the mock-treated cells, proving a complete rescue of the rapamycin-induced reduction of *cyclin D1* expression after PP2A inhibition (Fig. 6*B*).

Discussion

We have shown that GLI3, a transcriptional effector of SHH signaling, is regulated by PP2A activity and by the mTORC1 inhibitor rapamycin. Increased PP2A activity or mTORC1 inhibition led to both cytosolic translocation of full-length GLI3 and a reduction in its transcriptional activity toward its target gene *cyclin D1*, whereas reduced activity of PP2A led to a clear increase in the expression of *cyclin D1*. Strikingly, rapamycin achieved significant effects at concentrations corresponding to the low end of the therapeutic range used for organ-transplanted patients.

Subcellular localization of GLI3 but not GLI1 or GLI2 is regulated by PP2A activity and rapamycin. Significantly, localization of GLI3, but not GLI1 or GLI2, was affected by modulating PP2A activity and rapamycin treatment. This finding provides further evidence of the increased complexity of vertebrate SHH signaling compared with the *Drosophila* Hh pathway. Not only do multiple vertebrate homologues of Hh and Ci exist, but the activity of each of the Ci homologues (GLI1–GLI3) seems to be regulated via independent mechanisms. For example, GLI1 lacks an NH_2 terminal repressor domain that is present in both GLI2 and GLI3 (8, 28, 29). Moreover, GLI1, but not GLI3, can interact with cAMP-responsive element binding protein binding protein, which is a transcriptional coactivator in the SHH pathway that in *Drosophila* interacts with Ci (8). In addition, PKA-induced cleavage seems to exist for GLI3, but not for GLI1 or GLI2, in the mammalian system (8, 30, 31). Taken together, these data indicate that GLI3 is the actual functional orthologue of Ci and, by binding the GLI1 promoter region, acts as a master regulator of SHH signaling (8, 28). Indeed, manipulation of GLI3 subcellular localization and transcriptional activity in tumor cell lines is sufficient to significantly suppress the expression of the cell cycle regulator *cyclin D1*. Interestingly, among the tumor-related SHH target genes tested in this study, only *cyclin D1* responded to the knockdown of GLI3. It seems that SHH target gene expression and their control by a GLI3 transcriptional activator highly depends on the tissue context, which is consistent with previous observations (32, 33).

The transcriptional regulation of *cyclin D1*. Cyclin D1 is a major regulator of cell cycle progression and widely active in tumor

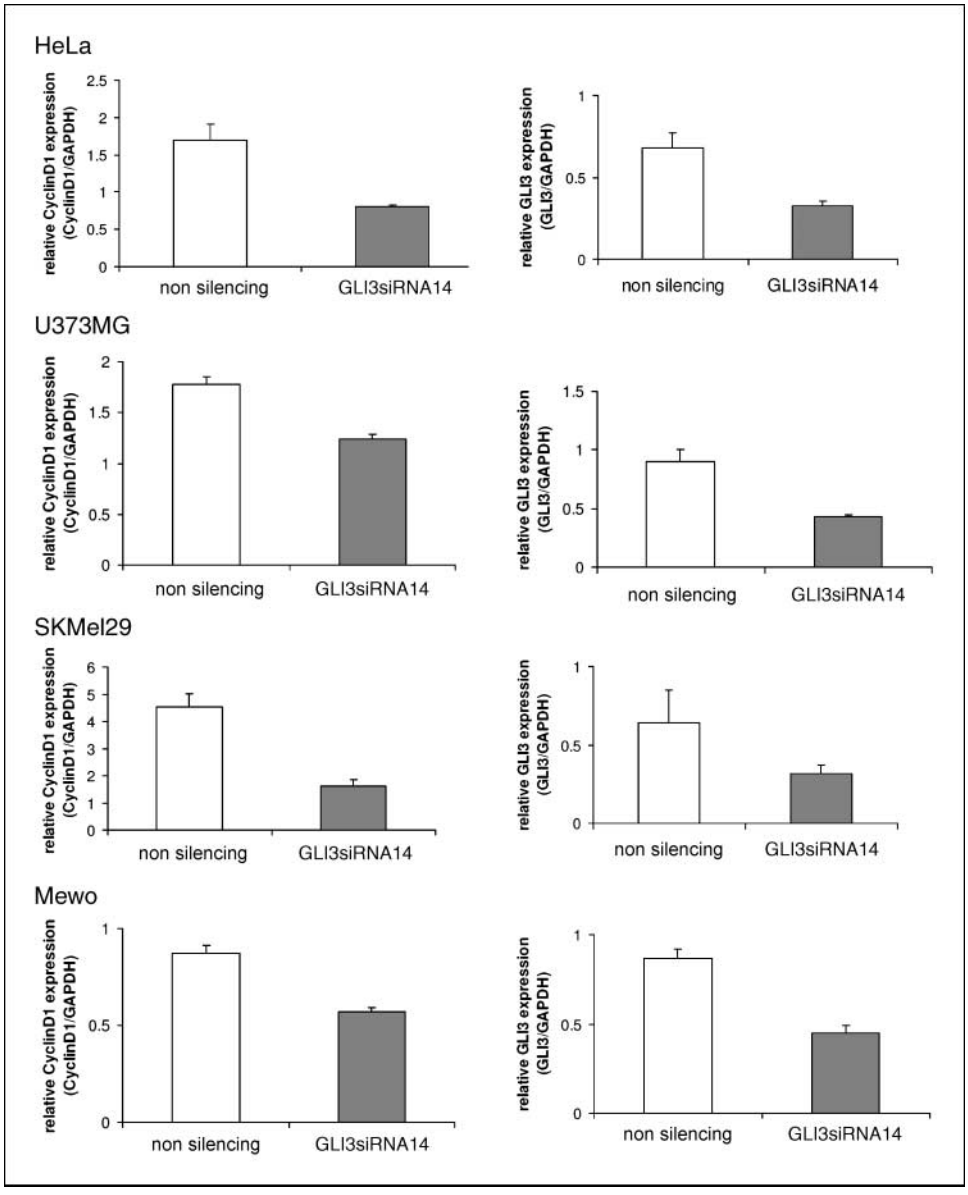

Figure 5. The transcriptional activity of endogenous GLI3 on cyclin D1. Relative mRNA amounts of *cyclin D1* (*left*) and *GLI3* (*right*) after transfection with nonsilencing siRNA (*white columns*) or GLI3-specific siRNA (*gray columns*) in HeLa, U373MG, SKMel29, and MeWo cells. *Columns,* mean values of four samples measured in parallel; *bars,* SD. Glyceraldehyde-3-phosphate dehydrogenase (GAPDH) was used for normalization.

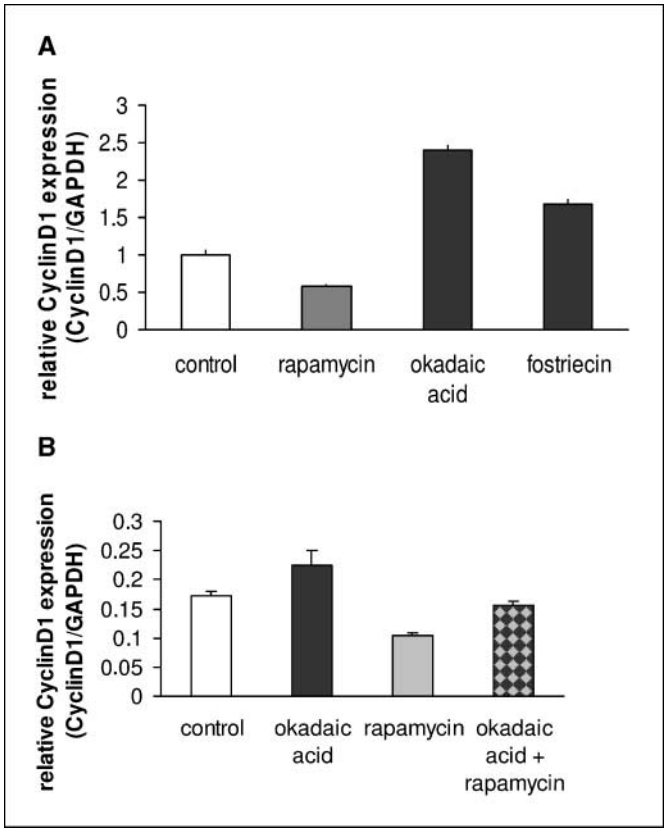

Figure 6. PP2A and rapamycin regulate the transcriptional activity of endogenous GLI3. *A,* relative mRNA amounts of *cyclin D1* in HeLa cells treated with rapamycin (*gray column*), okadaic acid, or fostriecin (*black columns*). *Columns,* mean values of four samples measured in parallel; *bars,* SD. GAPDH was used for normalization. *B,* relative mRNA amounts of *cyclin D1* in HeLa cells after rapamycin treatment (*gray column*), okadaic acid treatment (*black column*), or combined treatment with rapamycin and okadaic acid (*patterned column*).

formation and progression. Its transcriptional regulation is complex, involving at least four different transcription factor systems: the Wnt pathway (reviewed in ref. 34), nuclear factor-κB–related transcription factors (35–38), the activator protein 1 (AP-1) complex (39), and the SHH signaling cascade (23, 40–42). Using a GLI3-specific knockdown system, we showed here that, in several tumor cell lines with constitutively active SHH signaling, *cyclin D1* transcription critically depends on GLI3. Furthermore, we showed that GLI3-dependent regulation of *cyclin D1* transcription can be influenced by the mTORC1 inhibitor/PP2A activator rapamycin and the PP2A inhibitors okadaic acid and fostriecin. Thus, the present data identify activation of PP2A as a putative target for antineoplastic therapies.

Mechanisms underlying the antineoplastic activity of rapamycin. The immunosuppressant rapamycin interferes with tumorigenesis and has shown promising results as anticancer drug. Rapamycin derivatives are currently being evaluated in clinical trials for cancer therapy (reviewed in ref. 14). Interference with angiogenesis (43, 44) and inhibition of cell cycle progression through cyclin-dependent kinase activation (45) have been proposed as mechanisms for the anticancer effects of these drugs. In line with those actions, an effect of rapamycin on both mRNA and protein stability of cyclin D1 has been noted previously (46–48). The present data define a new mode of action of rapamycin as an antiproliferative antineoplastic agent: interference with the transcriptional induction of *cyclin D1* through inhibition of SHH signaling. Moreover, assays established in the present work, i.e., those involving regulation of GLI3 nuclear efflux, may be useful in screening for novel cell cycle inhibitors.

PP2A regulates SHH-dependent expression of *cyclin D1*. PP2A has been implicated in cellular growth control primarily based on the discovery that okadaic acid, an inhibitor of PP2A activity, is a potent tumor promoter (9). Whereas the mechanism underlying this observation remained elusive, it was shown that PP2A suppression leads to activation of the mitogen-activated protein kinase pathway in the absence of growth factor–initiated signaling, whereas PP2A is inactivated in response to cell growth stimulation (9, 49). Additionally, certain oncoproteins interact with PP2A, thus impairing its function (9), and specific PP2A complexes have been found to be up-regulated in transformed cells (49). PP2A also influences cell migration, as shown using a truncated form of its B56 subunit. The mutated B56 subunit seems to reduce the ability of PP2A to dephosphorylate components of focal adhesion complexes involved in adhesion spreading, migration, and invasion, all of which are cardinal features of malignant cells (reviewed in ref. 9), suggesting a role for PP2A as an endogenous suppressor of the metastatic phenotype.

Most recently, Tsuchiya and colleagues showed that the catalytic subunit of PP2A (PP2Ac) relocates to the nucleus in response to treatment with leptomycin B, causing inhibition of AP-1–dependent *cyclin D1* transcription, an effect that can be reversed by inhibitors of PP2A (22). In accord with their data, we now show that PP2A activity influences the subcellular localization of GLI3, an essential transcriptional effector in the SHH pathway and that changing the levels of PP2A activity modulates *cyclin D1* expression in a cell model with self-activated SHH signaling. In summary, our data help to close the gap between the observation that PP2A is a tumor suppressor and the molecular mechanisms behind it.

Disclosure of Potential Conflicts of Interest

No potential conflicts of interest were disclosed.

Acknowledgments

Received 11/9/2007; revised 3/5/2008; accepted 4/8/2008.

Grant support: Deutsche Forschungsgemeinschaft (SFB 577, project C04; Project SCHW 829/4-1), Volkswagen-Stiftung, and Special Research Program FWF-SFB021-"Cell Proliferation and Cell Death in Tumors" of the Austrian Science Fund (R. Schneider).

The costs of publication of this article were defrayed in part by the payment of page charges. This article must therefore be hereby marked *advertisement* in accordance with 18 U.S.C. Section 1734 solely to indicate this fact.

We thank Hannelore Madle and Susanne Freier for tissue culturing.

References

1. Wetmore C. Sonic hedgehog in normal and neoplastic proliferation: insight gained from human tumors and animal models. Curr Opin Genet Dev 2003;13:34–42.
2. Berman DM, Karhadkar SS, Maitra A, et al. Widespread requirement for Hedgehog ligand stimulation in growth of digestive tract tumours. Nature 2003;425:846–51.
3. Watkins DN, Berman DM, Burkholder SG, Wang B, Beachy PA, Baylin SB. Hedgehog signalling within airway epithelial progenitors and in small-cell lung cancer. Nature 2003;422:313–7.
4. Thayer SP, di Magliano MP, Heiser PW, et al. Hedgehog is an early and late mediator of pancreatic cancer tumorigenesis. Nature 2003;425:851–6.
5. Sanchez P, Hernandez AM, Stecca B, et al. Inhibition of prostate cancer proliferation by interference with SONIC HEDGEHOG-GLI1 signaling. Proc Natl Acad Sci U S A 2004;101:12561–6.
6. Murone M, Rosenthal A, de Sauvage FJ. Hedgehog

signal transduction: from flies to vertebrates. Exp Cell Res 1999;253:25–33.
7. Jacob J, Briscoe J. Gli proteins and the control of spinal-cord patterning. EMBO Rep 2003;4:761–5.
8. Dai P, Akimaru H, Tanaka Y, Maekawa T, Nakafuku M, Ishii S. Sonic Hedgehog-induced activation of the Gli1 promoter is mediated by GLI3. J Biol Chem 1999;274:8143–52.
9. Janssens V, Goris J, Van Hoof C. PP2A: the expected tumor suppressor. Curr Opin Genet Dev 2005;15:34–41.
10. Schmelzle T, Hall MN. TOR, a central controller of cell growth. Cell 2000;103:253–62.
11. Yang Q, Guan KL. Expanding mTOR signaling. Cell Res 2007;17:666–81.
12. Goldberg Y. Protein phosphatase 2A: who shall regulate the regulator? Biochem Pharmacol 1999;57:321–8.
13. Trockenbacher A, Suckow V, Foerster J, et al. MID1, mutated in Opitz syndrome, encodes an ubiquitin ligase that targets phosphatase 2A for degradation. Nat Genet 2001;29:287–94.
14. Bjornsti MA, Houghton PJ. The TOR pathway: a target for cancer therapy. Nat Rev Cancer 2004;4:335–48.
15. Peterson RT, Desai BN, Hardwick JS, Schreiber SL. Protein phosphatase 2A interacts with the 70-kDa S6 kinase and is activated by inhibition of FKBP12-rapamycinassociated protein. PNAS 1999;96:4438–42.
16. Inui S, Sanjo H, Maeda K, Yamamoto H, Miyamoto E, Sakaguchi N. Ig receptor binding protein 1† (α4) is associated with a rapamycin-sensitive signal transduction in lymphocytes through direct binding to the catalytic subunit of protein phosphatase 2A. Blood 1998;92:539–46.
17. Nanahoshi M, Nishiuma T, Tsujishita Y, et al. Regulation of protein phosphatase 2A catalytic activity by α4 protein and its yeast homolog Tap42. Biochem Biophys Res Commun 1998;251:520.
18. Murata K, Wu J, Brautigan DL. B cell receptor-associated protein α4 displays rapamycin-sensitive binding directly to the catalytic subunit of protein phosphatase 2A. Proc Natl Acad Sci U S A 1997;94:10624–9.
19. Hartley D, Cooper GM. Role of mTOR in the degradation of IRS-1: regulation of PP2A activity. J Cell Biochem 2002;85:304–14.
20. Mill P, Mo R, Hu MC, Dagnino L, Rosenblum ND, Hui CC. Shh controls epithelial proliferation via independent pathways that converge on N-Myc. Dev Cell 2005;9:293–303.
21. Li Y, Zhang H, Choi SC, Litingtung Y, Chiang C. Sonic hedgehog signaling regulates Gli3 processing, mesenchymal proliferation, and differentiation during mouse lung organogenesis. Dev Biol 2004;270:214–31.
22. Hu MC, Mo R, Bhella S, et al. GLI3-dependent transcriptional repression of Gli1, Gli2 and kidney patterning genes disrupts renal morphogenesis. Development 2006;133:569–78.
23. Weaver M, Batts L, Hogan BL. Tissue interactions pattern the mesenchyme of the embryonic mouse lung. Dev Biol 2003;258:169–84.
24. Walsh AH, Cheng A, Honkanen RE. Fostriecin, an antitumor antibiotic with inhibitory activity against serine/threonine protein phosphatases types 1 (PP1) and 2A (PP2A), is highly selective for PP2A. FEBS Lett 1997;416:230–4.
25. Kong M, Fox CJ, Mu J, et al. The PP2A-associated protein α4 is an essential inhibitor of apoptosis. Science 2004;306:695–8.
26. Donahue AC, Fruman DA. Distinct signaling mechanisms activate the target of rapamycin in response to different B-cell stimuli. Eur J Immunol 2007;37:2923–36.
27. Wyeth. Summary of product characteristics-rapamune: Wyeth Europe Ltd.; 2001.
28. Sasaki H, Nishizaki Y, Hui C, Nakafuku M, Kondoh H. Regulation of Gli2 and Gli3 activities by an amino-terminal repression domain: implication of Gli2 and Gli3 as primary mediators of Shh signaling. Development 1999;126:3915–24.
29. Bai CB, Joyner AL. Gli1 can rescue the *in vivo* function of Gli2. Development 2001;128:5161–72.
30. Wang B, Fallon JF, Beachy PA. Hedgehog-regulated processing of Gli3 produces an anterior/posterior repressor gradient in the developing vertebrate limb. Cell 2000;100:423–34.
31. Aza-Blanc P, Lin HY, Ruiz i Altaba A, Kornberg TB. Expression of the vertebrate Gli proteins in *Drosophila* reveals a distribution of activator and repressor activities. Development 2000;127:4293–301.
32. Buttitta L, Mo R, Hui CC, Fan CM. Interplays of Gli2 and Gli3 and their requirement in mediating Shh-dependent sclerotome induction. Development 2003;130:6233–43.
33. Vanderlaan G, Tyurina OV, Karlstrom RO, Chandrasekhar A. Gli function is essential for motor neuron induction in zebrafish. Dev Biol 2005;282:550–70.
34. Karim R, Tse G, Putti T, Scolyer R, Lee S. The significance of the Wnt pathway in the pathology of human cancers. Pathology 2004;36:120–8.
35. Guttridge DC, Albanese C, Reuther JY, Pestell RG, Baldwin AS, Jr. NF-κB controls cell growth and differentiation through transcriptional regulation of cyclin D1. Mol Cell Biol 1999;19:5785–99.
36. Hinz M, Krappmann D, Eichten A, Heder A, Scheidereit C, Strauss M. NF-κB function in growth control: regulation of cyclin D1 expression and G0/G1-to-S-phase transition. Mol Cell Biol 1999;19:2690–8.
37. Joyce D, Bouzahzah B, Fu M, et al. Integration of Rac-dependent regulation of cyclin D1 transcription through a nuclear factor-κB-dependent pathway. J Biol Chem 1999;274:25245–9.
38. von Wichert G, Haeussler U, Greten FR, et al. Regulation of cyclin D1 expression by autocrine IGF-I in human BON neuroendocrine tumour cells. Oncogene 2005;24:1284–9.
39. Shaulian E, Karin M. AP-1 in cell proliferation and survival. Oncogene 2001;20:2390–400.
40. Li Y, Zhang H, Choi SC, Litingtung Y, Chiang C. Sonic hedgehog signaling regulates Gli3 processing, mesenchymal proliferation, and differentiation during mouse lung organogenesis. Dev Biol 2004;270:214.
41. Mill P, Mo R, Hu MC, Dagnino L, Rosenblum ND, Hui C-c. Shh controls epithelial proliferation via independent pathways that converge on N-Myc. Dev Cell 2005;9:293.
42. Frost P, Shi Y, Hoang B, Lichtenstein A. AKT activity regulates the ability of mTOR inhibitors to prevent angiogenesis and VEGF expression in multiple myeloma cells. Oncogene 2006;26:2255–62.
43. Guba M, von Breitenbuch P, Steinbauer M, et al. Rapamycin inhibits primary and metastatic tumor growth by antiangiogenesis: involvement of vascular endothelial growth factor. Nat Med 2002;8:128–35.
44. Marx SO, Jayaraman T, Go LO, Marks AR. Rapamycin-FKBP inhibits cell cycle regulators of proliferation in vascular smooth muscle cells. Circ Res 1995;76:412–7.
45. Costa LJ. Aspects of mTOR biology and the use of mTOR inhibitors in non-Hodgkin's lymphoma. Cancer Treat Rev 2007;33:78–84.
46. Hashemolhosseini S, Nagamine Y, Morley SJ, Desrivieres S, Mercep L, Ferrari S. Rapamycin inhibition of the G1 to S transition is mediated by effects on cyclin D1 mRNA and protein stability. J Biol Chem 1998;273:14424–9.
47. Ong CT, Khoo YT, Mukhopadhyay A, et al. mTOR as a potential therapeutic target for treatment of keloids and excessive scars. Exp Dermatol 2007;16:394–404.
48. Chen W, Possemato R, Campbell KT, Plattner CA, Pallas DC, Hahn WC. Identification of specific PP2A complexes involved in human cell transformation. Cancer Cell 2004;5:127–36.
49. Tsuchiya A, Tashiro E, Yoshida M, Imoto M. Involvement of protein phosphatase 2A nuclear accumulation and subsequent inactivation of activator protein-1 in leptomycin B-inhibited cyclin D1 expression. Oncogene 2007;26:1522–32.